Engineering and Technology Journal
Journal homepage: engtechjournal.org

Extended Meshfree Approach for Crack Statistical Analysis of Anisotropic Functionally Graded Brazilian Disc Subjected to Traction Load

Hassanein I. Khalaf [a*], Haider K. Mehbes [b], Ameen A. Nassar [c]

[a] Mechanical Engineering Department, Basrah University, Basrah, Iraq, hassanein.khalaf@uobasrah.edu.iq

[b] Mechanical Engineering Department, Basrah University, Basrah, Iraq, haider.mehbes@uobasrah.edu.iq

[c] Mechanical Engineering Department, Basrah University, Basrah, Iraq, amen.nassar@uobasrah.edu.iq

*Corresponding author.

Submitted: 22/02/2020 Accepted: 01/05/2020 Published: 25/12/2020

K E Y W O R D S

Extended meshless method, orthotropic functionally graded disc, stress intensity factors.

A B S T R A C T

An extended meshless method that relying upon Galerkin formulation is applied on the crack analysis of orthotropic functionally graded Brazilian disc. Weak form is involved to solve the governing equation in the numerical method. In addition, enrichment terms and sub-triangle techniques are applied to improve the accuracy of relevant results. This paper depicts the influence of variation in the crack stretch and non-homogeneity parameters on the values of stress intensity factors using a developed MATLAB program. In the isotropic case, it is clear that when the length of crack increases, SIF increases. Graduation in E_{22} *has more effect in increasing the values of SIF in corresponding increased crack length. The verification has been checked by changing the range of the J-integral domain and variation of the support domain.*

How to cite this article: H. I. Khalaf, H. K. Mehbes, A. A. Nassar, "Extended meshfree approach for crack statistical analysis of anisotropic functionally graded brazilian disc subjected to traction load," Engineering and Technology Journal, Vol. 38, Part A, No. 12, pp. 1871-1879, 2020.

DOI: https://doi.org/10.30684/etj.v38i12A.1616

1. Introduction

Nowadays the Orthotropic Functionally Graded Materials (OFGM) has many uses and applications including in medical devices, vehicles, electronic equipment, etc. The properties of the relevant materials are changed in the directions of the body gradually. The first invention for these materials was in 1984 in Japan [1]. There are abundant of researchers that deliberated crack analysis and fracture mechanism in FGMs numerically. F. Delale and F. Erdogan [2] studied the crack problem in non-homogeneous plates via using finite elements. J.E. Dolbow and M. Gosz [3] calculated mixed mode SIFs in FGMs. B.N. Rao and S. Rahman [4] used the meshfree method to extract SIFs of mixed FGMs problems. J.-H. Kim and G. H. Paulino [5,6] presented the formulation of the extract M-integral in FGMs using the finite element method in various examples. K. Y. Dai et al. [7] applied the meshfree radial point interpolation method to find SIFs in FGMs. J. Sladek et al. [8] employed the meshless local technique to determine the stress intensity factors in the related materials. H. Khazal et al. [9], and H. Khazal and N. Saleh [10] developed a meshfree method and then applied it to find SIFs in FGM. Hassanein Ibraheem et al. [11] applied XEFGM to find the SIFs in FGM under thermal load. All these researchers have not studied the effect of the increase of crack length on the SIFs for orthotropic and isotropic FGMs. On the other hand, few researchers used optical techniques to analyze the fracture problems in the related materials [12-16]. Therefore, in this work extended meshless method is employing that relying upon Galerkin formulation XEFGM for crack analysis of OFG Brazilian disc subjected to compression load. Besides, originality of this research enrichment terms and sub-triangle forms are applied to improve the relevant results. Further, this paper depicts the influence of variation in crack length, load, and non-homogeneity parameters on the values of stress intensity factors using a developed MATLAB program.

2. Extended meshless method

Figure 1 illustrates a 2D orthotropic functionally graded body which represents a crack Γ_c. There is no finite element in the representation of the domain of the meshless numerical method. Rather than finite element, the support domain is utilized in an extended meshless method that relying upon Galerkin formulation XEFGM. The weak form of governance formula may be labeled as [17]:

$$\int_{\Omega} (L\delta u)^T (DLu) d\Omega - \int_{\Omega} \delta u^T b d\Omega - \int_{\Gamma_t} \delta u^T \bar{t} d\Gamma - \int_{\Gamma_u} \delta \lambda^T (u-\bar{u}) d\Gamma - \int_{\Gamma_u} \delta u^T \lambda d\Gamma = 0 \quad (1)$$

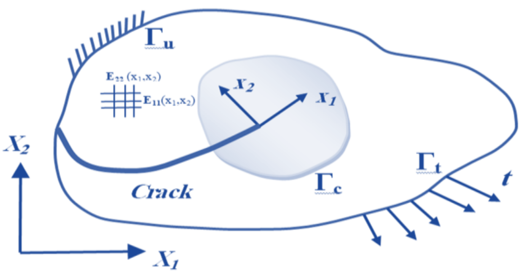

Figure 1: 2D orthotropic functionally graded body

A good enrichment formula [9] has been utilized to capture all the discontinuity terms in the region of crack that representing in the displacement field:

$$u^h(\mathrm{x}) = \sum_{i=1}^{n} \phi_i(\mathrm{x}) u_i + \sum_{k=1}^{m_t} \phi_k \sum_{\alpha=1}^{4} Q_\alpha(\mathrm{x}) s_k \quad (2)$$

where $\boldsymbol{s}_k$ is the inbound of a supplementary grade of freedom for molding crack tips m_t. Where $\phi_i(\mathrm{x})$ is a shape function, which determined by depending on the moving least square method [17,18]. Solving of Eq. (1) results in

$$\begin{bmatrix} \mathrm{K} & \mathrm{Q} \\ \mathrm{Q^T} & 0 \end{bmatrix} \begin{bmatrix} \mathrm{U} \\ \lambda \end{bmatrix} = \begin{bmatrix} \mathrm{F} \\ \mathrm{q} \end{bmatrix} \quad (3)$$

Where

$$\mathrm{Q} = -\int_{\Gamma_u} \mathrm{N^T} \phi \, d\Gamma \quad (4)$$

$$q = -\int_{\Gamma_u} N^T \bar{u}\, d\Gamma \tag{5}$$

$$\lambda(x) = \sum_{i=1}^{n_\lambda} N_i(x)\lambda_i \tag{6}$$

$$U = \{u \quad s1 \quad s2 \quad s3 \quad s4\}^T \tag{7}$$

$$K_{ij}^n = \begin{bmatrix} K_{ij}^{uu} & K_{ij}^{ub} \\ K_{ij}^{bu} & K_{ij}^{bb} \end{bmatrix} \tag{8}$$

$$F_i^n = \{F_i^u \quad F_i^{b_1} \quad F_i^{b_2} \quad F_i^{b_3} \quad F_i^{b_4}\}^T \tag{9}$$

$$K_{ij}^{rs} = \int_\Omega (B_i^r)^T D B_j^s\, d\Omega \quad (r, s = u, b) \tag{10}$$

$$F_i^u = \int_\Omega \phi_i^t b\, d\Omega + \int_{\Gamma_t} \phi_i^T \bar{t}\, d\Gamma \tag{11}$$

$$F_i^{ba} = \int_\Omega \phi_i^T Q_a b\, d\Omega + \int_{\Gamma_t} \phi_i^T Q_a \bar{t}\, d\Gamma \quad (a = 1,2,3,4) \tag{12}$$

$$B_i^u = \begin{bmatrix} \phi_{i,x} & 0 \\ 0 & \phi_{i,y} \\ \phi_{i,y} & \phi_{i,x} \end{bmatrix} \tag{13}$$

$$B_i^b = \begin{bmatrix} B_i^{b_1} & B_i^{b_2} & B_i^{b_3} & B_i^{b_4} \end{bmatrix} \tag{14}$$

$$B_i^u = \begin{bmatrix} (\phi_i Q_\alpha)_{,x} & 0 \\ 0 & (\phi_i Q_\alpha)_{,y} \\ (\phi_i Q_\alpha)_{,y} & (\phi_i Q_\alpha)_{,x} \end{bmatrix} (\alpha = 1,2,3,4) \tag{15}$$

Strain and stress may thereafter be found for u^h employing Eqs. (16) and (17), consecutively,

$$\varepsilon = Lu^h \tag{16}$$

$$\sigma = D\varepsilon \tag{17}$$

3. Stress intensity factor determination

The interaction whole formula is utilized to extract stress intensity factors (SIFs) [19]:

$$M = \int_A \left\{\sigma_{ij}\, u_{i,1}^{aux} + \sigma_{ij}^{aux} u_{i,1} - \frac{1}{2}(\sigma_{ik}\varepsilon_{ik}^{aux} + \sigma_{ik}^{aux}\varepsilon_{ik})\delta_{1j}\right\} q_{,j}\, dA \; + \int_A \left\{\sigma_{ij}(c_{ijkl}^{tip} - c_{ijkl}(x))\sigma_{kl,1}^{aux}\right\} q\, dA \tag{18}$$

Two superimposed fields can be represented as

$$M = 2t_{11}K_I^{aux} K_I + t_{12}(K_I^{aux}K_{II} + K_{II}^{aux}K_I) + 2t_{22}K_{II}^{aux}K_{II} \tag{19}$$

with

$$t_{11} = -\frac{c_{22}}{2}\,\mathrm{Im}\left(\frac{S_1+S_2}{S_1S_2}\right) \tag{20}$$

$$t_{12} = -\frac{c_{22}}{2}\,\mathrm{Im}\left(\frac{1}{S_1S_2}\right) + \frac{c_{11}}{2}\,\mathrm{Im}(s_1s_2) \tag{21}$$

$$t_{22} = -\frac{c_{11}}{2}\mathrm{Im}(s_1 + s_2) \tag{22}$$

Where s_1 and s_2 are the roots of the trait approach of the orthotropic cracked body; while c_{ij} is an ingredient of compliance matrix **C**. More details on the relevant meshfree method, enrichment functions, and M-integral can be determined in [9].

Substituting $K_I^{aux} = 1, K_{II}^{aux} = 0$ and $K_I^{aux} = 0, K_{II}^{aux} = 1$ into (19), gives

$$M_1 = 2t_{11}K_I + t_{12}K_{II} \qquad (K_I^{aux} = 1, K_{II}^{aux} = 0) \tag{23}$$

$$M_2 = t_{12}K_I + 2t_{22}K_{II} \qquad (K_I^{aux} = 0, K_{II}^{aux} = 1) \tag{24}$$

The two last equations can be solved to find SIFs.

4. Sub-triangles technique

The sub-triangles technique is employing in the crack region to enhance the precision of the integration process and finally to have the best results for the values of SIF. The background cell of any sub-triangle is imposed by 13 integrated points at the crack surface and tip. Moreover, six and four voided sub-triangle cells are distributed in the background cells of the crack tip and crack surface respectively as shown in Figure 2. The background cells are used for the integration of the numerical equations using the Gauss quadrature method.

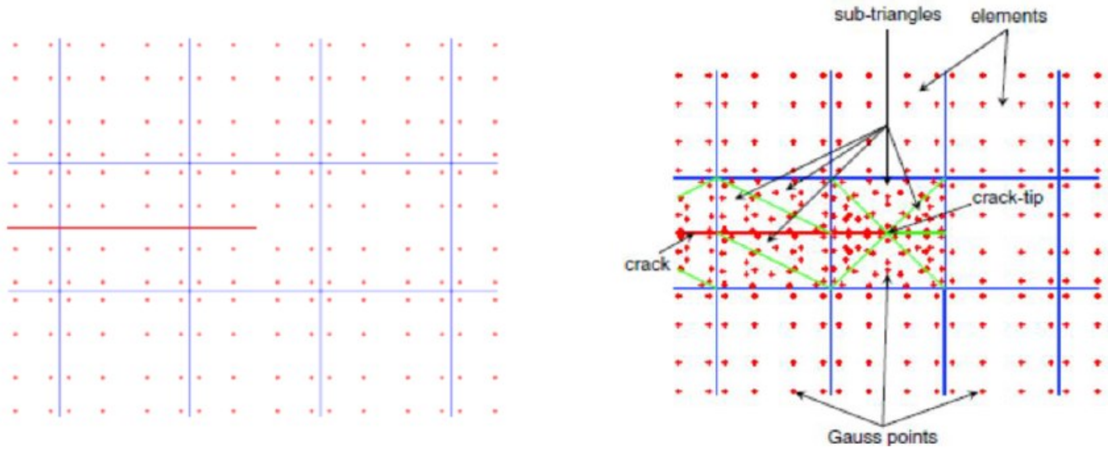

Figure 2: Integration points in the crack region in classical method and in sub-triangles form

5. Case study-anisotropic functionally graded Brazilian disc subjected to traction point load

Few researchers studied the crack analysis of the FG Brazilian disc under traction load such as [9,20] but these references debated only the fracture analysis of the FG Brazilian disc under fixed crack length. The current paper depicts the effect of variation in the crack extent and in non-homogeneity parameters (α, β, γ) on the values of stress intensity factors using a developed MATLAB program. The case, illustrated in Figure 3, displays a disc a crack tending by θ=30º. The disc is subjected to traction load P=±100 N/m. The gradations of material properties with are explained as,

$$E_{11}(r) = E_{11}^{O}\, e^{\alpha r}, E_{22}(r) = E_{22}^{O}\, e^{\beta r}, G_{12}(r) = G_{12}^{O}\, e^{\gamma r} \tag{25}$$

$$r = \sqrt{X_1^2 + X_2^2} \tag{26}$$

and,

$$E_{11}^{O} = 0.1\,, E_{22}^{O} = 1.0\,, G_{12}^{O} = 0.5, \upsilon_{12} = 0.03$$

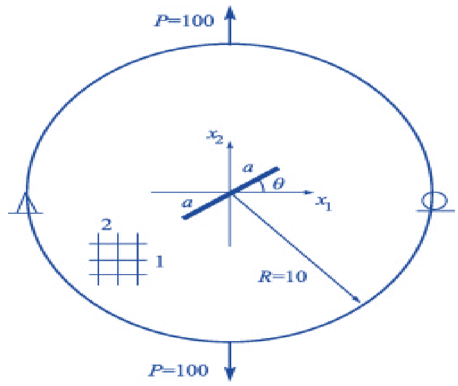

Figure 3: FG Brazilian disc under traction load

The total number of nodes is 989 as shown in Figure 4. The circle of J-integral radius and background cells can be seen in Figure 5. In addition, the gauss scattering describes in Figure 6; 3 gauss points are used by applying the sub-triangle technique nearby the crack tip and crack surface.

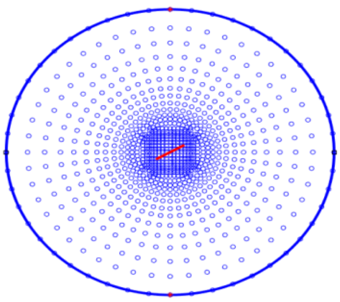

Figure 4: nodal distribution of the problem

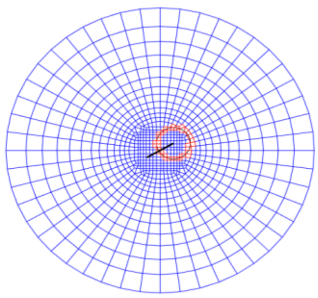

Figure 5: background cells distribution

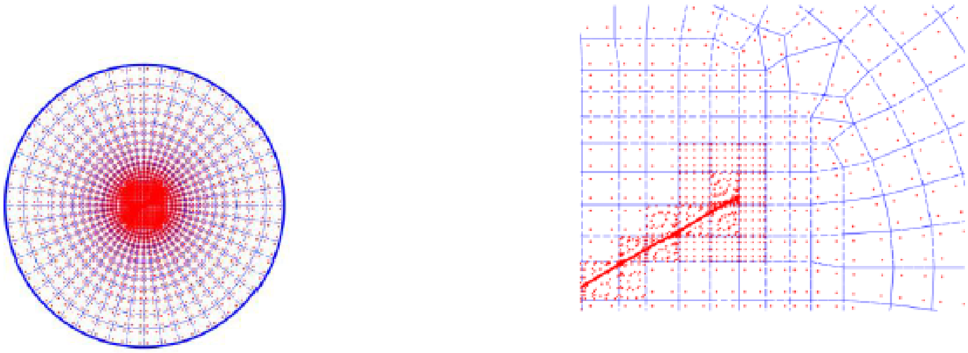

Figure 6: Gauss scattering for whole domain and for zoom in the right crack tip

In the isotropic case, Table I clears the influence of crack length on the SIFs. It is evident that when the length of crack increases, SIF increases.

TABLE I: crack length vs. SIFs (Mpa. $\sqrt{m}$) at radial gradation β=α=γ=0, r_J=1.6/a.

a (d_{max} =1.7)	K_I	K_{II}	K_I [9]	K_{II} [9]	K_I [20]	K_{II} [20]
1	12.11	17.11	11.33	16.73	12.11	17.11
1.25	17.65	12.93	--	--	--	--
1.5	15.05	22.06	--	--	--	--
1.75	15.83	23.91	--	--	--	--

Table II describes orthotropic FG cases for different non-homogeneity terms βa=αa=γa. Obviously, if non-homogeneity parameters are positive and equal, there is a very slight effect on the results of SIFs at various crack lengths. It is evident that when non-homogeneity parameters rise, SIF reduces mightily.

TABLE II: describes orthotropic FG cases for different non-homogeneity terms βa=αa=γa.

a	βa	K_I	K_{II}	K_I [9]	K_{II} [9]	K_I [20]	K_{II} [20]
1	-0.5	28.58	19.12	28.58	18.56	29.22	19.12
1.25	-0.5	39.39	26.08	--	--	--	--
1.5	-0.5	54.25	39.09	--	--	--	--
1	0.5	<u>5.76</u>	<u>3.75</u>	5.76	3.847	5.459	3.75
1.25	0.5	<u>5.63</u>	<u>3.56</u>	--	--	--	--
1. 5	0.5	<u>5.31</u>	<u>3.40</u>	--	--	--	--

Table III shows orthotropic FG cases for different non-homogeneity parameters. where if crack length increases, SIFs increases. Further, when graduating in E_{22} only (αa=0.0, βa=0.1, γa=0.0), $\mathbf{K_I}$ results have a slightly more increase than other relevant results in else cases.

TABLE III: SIFs (Mpa. $\sqrt{m}$) for various crack lengths and non-homogeneity parameters at dmax =1.7, rJ=1.6/a.

a	Non-homogeneity parameters	K_I	K_{II}	K_I [20]	K_{II} [20]
1	αa=0.1, βa=0.0,γa=0.0	15.25	11.05	10.42	15.45
1.25	αa=0.1, βa=0.0,γa=0.0	17.33	12.13	--	--
1.5	αa=0.1, βa=0.0,γa=0.0	19.58	13.45	--	--
1	αa=0.0, βa=0.1,γa=0.0	17.87	12.05	17.08	11.50
1.25	αa=0.0, βa=0.1,γa=0.0	19.45	12.99	--	--
1.5	αa=0.0, βa=0.1,γa=0.0	21.53	13.90	--	--
1	αa=0.0, βa=0.0,γa=0.1	15.90	11.16	16.73	11.33
1.25	αa=0.0, βa=0.0,γa=0.1	17.77	12.76	--	--
1.5	αa=0.0, βa=0.0,γa=0.1	20.08	14.05	--	--

Table IV and Figure 7 describe the insensitivity of SIFs in rapprochement with variation in the magnitudes of d_{max} and r_J respectively.

TABLE IV:SIFs (Mpa. $\sqrt{m}$) vs. size of support domain dmax at αa=0.1, βa=0.0, γa=0.0, a=1.5, r_J=1.6/a.

dmax	KI	KII
1.5	19.32	12.81
1.7	19.57	13.45
1.9	19.81	13.87
2.2	20.07	14.04

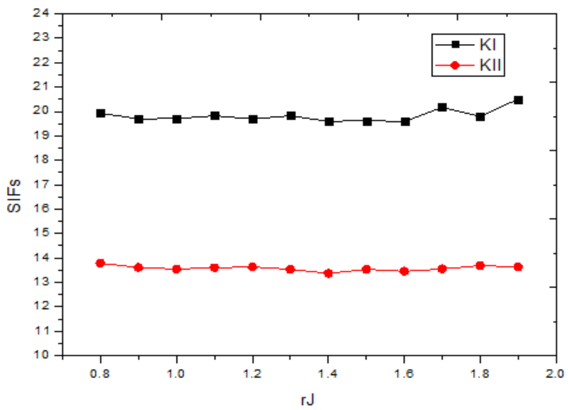

Figure 7: SIFs (Mpa. $\sqrt{m}$) vs. r_J/a at αa=0.1, βa=0.0, γa=0.0, a=1.5, d_{max} =1.7.

6. Conclusions

In this research a numerically crack analysis in OFGM Brazilian disc that subjected to traction load be done. The extended element free Galerkin method have well powerful in the solution of the fracture problems. It is clear that the change of the crack length has a clear effect on the SIFs results at different non-homogeneity parameters of the gradation of the relevant material. The important thing to be mentioned that the selection of positive and constant non-homogeneity parameters in all directions reduces evidently the results of the SIFs. Further, in orthotropic FG cases for different non-homogeneity parameters, when graduation in E_{22} only (αa=0.0, βa=0.1, γa=0.0), KI results have a slightly more increase than other relevant results in else cases. Briefly, the significant points of the conclusions of this research can be remarked as follow:

1) In the isotropic case, it is manifest that when the length of crack increases, SIF increases.

2) In non-homogeneity parameters are positive and equal, there is a very small influence on the results of SIFs at various crack lengths.
3) When these parameters are negative and equal, there are huge increases in the SIFs with the increase of the crack length.
4) Graduation in E_{22} has more effect in increasing the values of SIFs in corresponding crack length.

An extension to dynamic orthotropic XEFG under thermal load is powerfully aimed for interesting crack analysis of related materials.

Nomenclature

E: Modulus of elasticity (Young's Modulus), MPa
G: Shear modulus, MPa
M: Interaction integral, N/m
N: number of nodes
a: The length of a crack, mm
b: Body force, N
d_{ml}: variation of the support domain, m
n: variation of the support domain
n_j: The unit outward normal to contour
r: Radial distance from a crack tip, m
rJ: Size of J-Integral, m
$\bar{t}$: traction force, N
t: Time, s
u^h: The unknown trial approximation of displacement, m
$\bar{u}$: The prescribed displacements on the boundary, m
w: The weight function of an influence node
Ω: The global domain of the problem
Γ: Boundary of the global domain
δ: Kronecker delta
ϕ: Shape function
ν: Poisson's ratio
κ: Kolosov constant
ρ: Mass density, kg/m^3
λ: Lagrange multiplier

Matrices and Vectors

a: The vector of unknown coefficients
b: The body forces vector
B_j: Shape function derivatives matrix
D: Material properties "constitutive" matrix
F: Force vector
K: Stiffness matrix
L: The differential operator matrix
M: Mass matrix
P: Basis vector
S: Compliance matrix
$\bar{t}$: Traction vector
u: Displacement vector
x: Nodal position vector
Φ: Shape function matrix
$\mathcal{E}$: Strain vector
σ: Stress vector

References

[1] I. Shiota and Y. Miyamoto, "Functionally graded materials 1996", Elsevier Science, proceedings of the 4th international symposium on Functionally Graded Materials," AIST Tsukuba Research center, Tsukuba, Japan, pp.21-24, October,1996.

[2] F. Delale and F. Erdogan, "The crack problem for a non-homogeneous plate," ASME Journal of Applied Mechanics, Vol.50, No.3, pp.609–614, 1983.

[3] J. E. Dolbow and M. Gosz, "On the computation of mixed-mode stress intensity factors in integral and micromechanics models," International Journal for Numerical Methods in Engineering, Vol. 58, pp.1457–1497, 2003.

[4] B. N. Rao and S. Rahman, "Mesh-free analysis of cracks in isotropic functionally graded materials," Engineering Fracture Mechanics, Vol.70, pp.1–27, 2003.

[5] J. H. Kim and G. H. Paulino, "An accurate scheme for mixed-mode fracture analysis of functionally graded materials using the interaction of the Interaction Integral Method for Fracture of Functionally Graded Materials," Journal of Applied Mechanics, ASME, Vol. 72, pp 351-364, May, 2005.

[6] J. H. Kim and G. H. Paulino, "Consistent Formulations functionally graded materials," International Journal of Solids and Structures, Vol. 39, pp.2557–2574, 2002.

[7] K. Y. Dai, G. R. Liu, K. M. Lim, X. Han and S. Y. Du, "A meshfree radial point interpolation method for analysis of functionally graded material (FGM) plates," Computational Mechanics, Vol.34, Springer-Verlag, pp.213–223, 2004.

[8] J. Sladek, V. Sladek and C. Zhang, "A meshless local boundary integral equation method for dynamic anti-plane shear crack problem in functionally graded materials," Engineering Analysis with Boundary Elements, Vol.29, pp.334–342, 2005.

[9] H. Khazal, H. Bayesteh, S. Mohammadi, S. S. Ghorashi, and A. Ahmed, "An extended element free Galerkin method for fracture analysis of functionally graded material," Mech. Adv. Mater. Struct., Vol.23, pp.513–528, 2016.

[10] H. Khazal, and N. Saleh, "XEFGM for crack propagation analysis of functionally graded materials under mixed-mode and non-proportional loading," Mech. Adv. Mater. Struct. Vol.11, No.11, pp.975–983, 2019.

[11] H. Ibraheem, H. Khazal, and A. Ahmed, "Steady State Thermo XFEM Fracture Analysis of Isotropic and an Isotropic FG Plate with Inclined Center Crack," Basrah Journal for Engineering Sciences, Vol. 18, No.1, 201

[12] R. J. Butcher, C.-E. Rousseau and H. V. Tippur, "A functionally Graded Composite: Preparation, Measurements and Failure Analysis," Acta mater. Vol. 47, No. 1, pp. 259-268, 1999.

[13] L. Lambros, A. Narayanaswamy, M. H. Santare, G. Anlas, "Manufacture and Testing of a Functionally Graded Material," ASME, Vol.121, Oct., 1999.

[14] C. E. Rousseau and H. V. Tippur, "Compositionally Graded Materials with cracks normal to the elastic gradient," Department of Mechanical Engineering, 202 Ross Hall, Auburn University, Auburn, AL 36849, USA, Acta Metallurgica , Elsevier Science, 2000.

[15] W. Farouq, H. Khazal, and A. K. F. Hassan, "Fracture analysis of functionally graded material using digital image correlation technique and extended element-free Galerkin method," Optics and Lasers in Engineering, Vol. 121, pp.307-322, October, 2019.

[16] H. Khazal, A. Hassan, W. Farouq, and H. Bayesteh, "Computation of Fracture Parameters in Stepwise Functionally Graded Materials Using Digital Image Correlation Technique," Materials Performance and Characterization", Vol.8, No. 1, pp.344-354, 2019.

[17] G. R. Liu, "Meshfree methods moving beyond the finite element method," second edition- by Taylor and Francis Group, LLC, 2010.

[18] P. Lancaster and K. Salkauskas, "Surfaces generated by moving least squares methods," Mathematics of Computation, Vol. 37, pp. 141-158, 1981

[19] J. H. Kim and G. H. Paulino, "Mixed-mode fracture of orthotropic functionally graded materials using finite elements and the modified crack closure method," Engineering Fracture Mechanics, Vol.69, pp.1557–1586, 2002.

[20] J. H. Kim and G. H. Paulino, "The interaction integral for fracture of orthotropic functionally graded materials: Evaluation of stress intensity factors," Int. J. Solids Struct., Vol. 40, pp. 3967–4001, 2003.